ENHANCED ELECTRO-OSMOTIC PUMPING WITH LIQUID BRIDGE AND FIELD EFFECT FLOW RECTIFICATION

Senol Mutlu[1], Frantisek Svec[2], Carlos H. Mastrangelo[3],
Jean M.J. Fréchet[2] and Yogesh B. Gianchandani[1]

[1]Department of Electrical Engineering and Computer Science, University of Michigan,
Ann Arbor, MI 48109-2122, USA
[2]Department of Chemistry, University of California, Berkeley, CA 94720-1462, USA
[3]Corning IntelliSense Corporation, Wilmington, MA 01887, USA

ABSTRACT

We have previously demonstrated that polymer plugs with sub-micron pores can suppress unwanted pressure-driven flow and enhance electro-osmotic flow in a microchannel. This paper presents two separate concepts related to electrode placement and biasing strategy that further abate generation of bubbles in the main flow. In the first concept the drive signal is applied to a main EOF porous plug through high flow resistance porous bridges present outside the main flow. In the second approach, metal electrodes are located within the main channel across a series of dielectrically isolated narrow channels. Bubble generation is suppressed with a high-frequency square wave drive, and net unidirectional flow is achieved by modulation of the zeta potential on the narrow channel surfaces. Flow velocities of 10-66 μm/sec in 20-μm high channels have been achieved by these two methods.

I. INTRODUCTION

Most solid surfaces such as metal, polymer and glass, acquire a finite charge density at the interface upon contact with a *polar* liquid. For the case of glass-water interface, the surface is charged due to the deprotonation of surface silanol groups [1]. The charged surface attracts counter-ions and repels co-ions in the solution. Deprotonation usually leaves the solid surface negatively charged, causing the surface to attract positive ions in the solution. A double layer of ions is formed, consisting of a compact immobile layer and a mobile diffuse layer in the liquid. If an electric field is applied parallel to the interface, mobile charges in the diffuse layer are moved, (dragging the liquid with them) while charges in the compact layer remain immobile (Fig. 1). This movement of liquid as a result of the electric field is called the electro-osmotic flow (EOF).

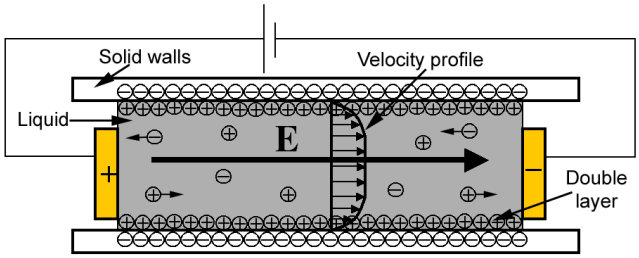

Fig. 1: Depiction of electro-osmotic flow

Electro-osmotic pumps are attractive in fluidic microsystems for polar liquids because they have no moving parts and can be integrated easily. A simple calculation [2] shows that channel dimensions must be less than 1 μm to generate adequate pressure heads with low voltage EOF pumps. Previously we have achieved this by driving EOF through polymer plugs with average pore diameter of ≈300 nm inside parylene channels [3].

In these devices electrode placement and biasing schemes play a critical role in the EOF velocity. These parameters must be used judiciously to maximize EOF while suppressing generation of electrolytic gas bubbles that obstruct flow. Bubble suppression has been reported previously using an asymmetric low frequency zero net charge current signal applied directly across the porous plug [3]. In this scheme, unidirectional flow is achieved through Faradaic rectification [4] of the corresponding time averaged plug voltage. Flow velocities of 16 μm/s were achieved with maximum velocities limited by the nonlinearity of the plug *IV* characteristic.

This paper presents two additional biasing approaches. The first approach relies on placement of electrodes outside of the flow, and the second uses modulation of the zeta potential.

II. DC DRIVE THROUGH LIQUID BRIDGES

The detrimental effects of bubbles can be eliminated if bubbles are generated outside the main flow path. This can be achieved by placing electrodes outside the main flow channel as shown in Fig. 2. The electric field is then applied to the main porous plug through narrow liquid bridges. To be effective, these bridges must have low electrical resistance but high flow impedance. The use of gelatinous liquid bridges in EOF pumps has been discussed by Takamura [5,6]. Takamura used a long series of narrow, necked channel regions to provide high resistance to pressure driven flow. Biasing of the channel was provided through a conductive gel. In this paper we use a short porous polymer plug embedded in the main channel, making this implementation compact and suitable for microfluidic chips that require multi pump configurations. Net pumping in these devices is generated through a difference in the effective electro-osmotic mobility between

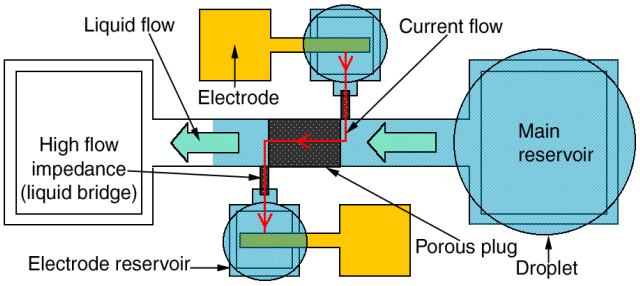

Fig. 2: Schematic of porous plug electro-osmotic pump (Pp-EOP) with liquid bridge connections.

nanochannels of the various porous plugs and the main channel.

The effect of using porous bridges is next examined. A porous structure can be modeled as a packing of parallel cylindrical channels with a radius a. To characterize a porous structure, two new parameters must be defined: tortuosity, τ, and porosity, Ψ. Tortuosity is defined as $\tau = (L_e / L)^2$, where L_e is the average length of travel for flow along the pore path and L is the physical length of the porous structure. Porosity is defined as $\Psi = U_e / U$, where U_e is the void volume and U is the total volume of the porous structure. The effective cross-sectional area of the porous structure can be estimated as $A_e = \Psi WL / \sqrt{\tau} = \Psi A / \sqrt{\tau}$, where W is the physical width and A is the physical cross-sectional area of the porous structure [7]. The electrical resistance of the porous polymer with a liquid of resistivity, ρ_l, in its pores is:

$$R_{el} = \frac{\rho_l L \tau}{\Psi A} \quad (1)$$

Similarly, a hydraulic resistance can be defined for the liquid flow in micro domain since the Reynolds number is low and the liquid flow is laminar. This means pressure drop along a channel is proportional to the volume flow rate. The hydraulic resistance for the porous structure can be inferred from that of a single capillary and is given by:

$$R_{hyd} = \frac{8\eta L \tau}{a^2 \Psi A} \quad (2)$$

where η is the viscosity of the liquid and a is the radius of the pore. For this porous polymer a=150 nm, τ=2, Ψ=0.6. To evaluate the significance of having a porous polymer in the channel, the flow in a channel with a radius of 15-µm is examined in the presence and absence of the porous plug. Having the plug increases the electrical resistance only 3.3 times. However, the hydraulic resistance increases 10,000 times, effectively blocking pressure driven flow.

Devices were fabricated with a four-mask surface micromachining process described in [3]. The polymer used was the product of polymerization of a mixture of ethylene dimethacrylate, butyl methacrylate and propenasulfonic acid in the presence of a porogenic solvents consisting of propanol, butanediol and water. Figure 3 shows a fabricated device. Devices were tested with DI water in equilibrium with atmospheric carbon dioxide. Figure 4 shows the forward and reverse liquid

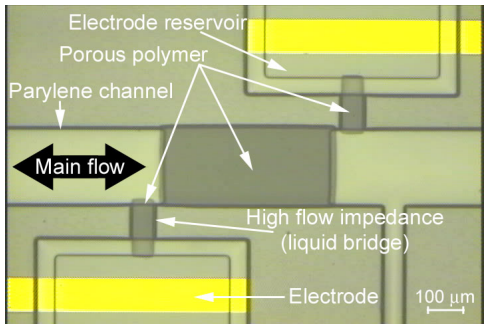

Fig. 3: Top view of the fabricated Pp-EOP with liquid bridge.

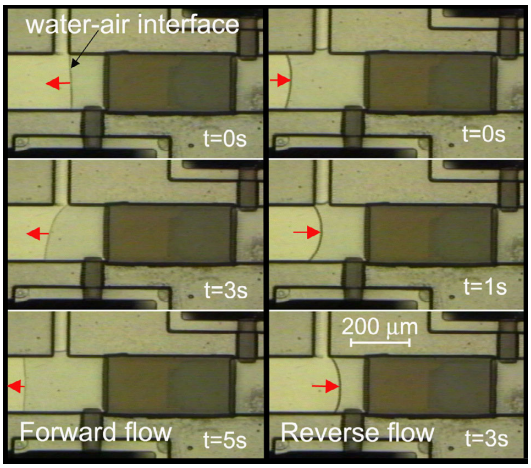

Fig. 4: Forward and reverse water-air interface movement with DC voltage applied and polarities reversed respectively.

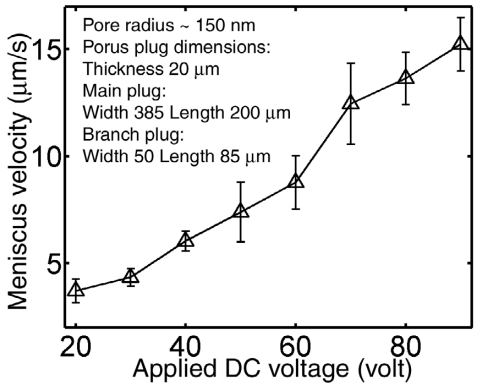

Fig.5: Water-air interface velocity versus applied DC voltage.

flow in the main channel when a DC voltage is applied and reversed, respectively. Measured results of water-air interface velocities with different DC voltage magnitudes are in Fig. 5. Velocity increased linearly with the applied voltage. At 50 volt DC, the maximum volume flow rate, Q_{max}, was 1.76 nL/min, which was calculated by multiplying the meniscus velocity by the cross-sectional area of the channel (200x20 µm^2). It was maximum because the measurements were made with the flow facing zero pressure. Calculated hydraulic resistances of porous plugs are around 1.14x10^{17} Pa.s/m^3. A suitable figure of merit is the ratio of zero-flow pressure head per unit voltage per real estate area of the device. Zero-flow pressure head can be estimated from $P_{max}=Q_{max} R_{hyd}$. Takamura's device

yields a figure of merit of 4.2 x10^{-4} PaV^{-1} μm^{-2} while this device yields an estimated 3.7 x10^{-4} $PaV^{-1}\mu m^{-2}$.

III. AC DRIVE WITH FIELD EFFECT RECTIFICATION

The zeta potential of a fluid in a micro-channel can be altered by a bias applied to an insulated channel wall thus permitting the direction of electro-osmotic flow to be reversed [8]. We use this concept with a high aspect ratio, perforated metal gate electrode coated with an insulator, as a substitute for the porous plug in the electro-osmotic pump (Fig.6). The gate electrode is driven synchronously with in-channel metal electrodes, up-stream and down-stream of it, to achieve unidirectional flow. Since the drive electrodes are inside the main channel, a high frequency zero averaged AC voltage (V_d) is applied to prevent bubble generation. Without the gate electrode, this would result in net zero movement. However, if the negative of the AC signal is applied to the gate electrode (V_g) the zeta potential is synchronously modulated in the negative half-cycle, and the flow is rectified (Fig. 7). This effect resembles AC electro-osmosis where this kind of zeta potential modulation happens on a metal surface [9]. Other cases are summarized in Table 1.

One question that arises for this approach is if EOF can respond to alternating electric fields at high frequencies. The time necessary for the liquid to assume this slip velocity after the application of the electric field can be calculated from $t_{char}=a^2 d/5.8\eta$, where a is the radius of the channel and d is the density of the liquid [10]. For a 13-µm channel radius this value is 30 µs or 34 KHz.

Fabrication process for the device is shown in Fig. 8.

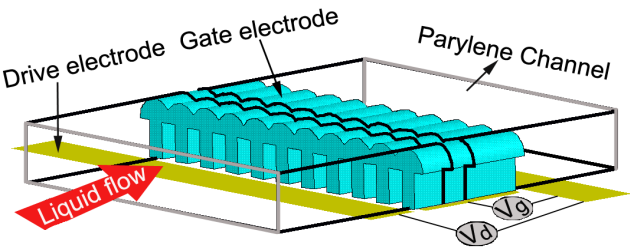

Fig.6: Schematic of a new flow field effect transistor (flowFET).

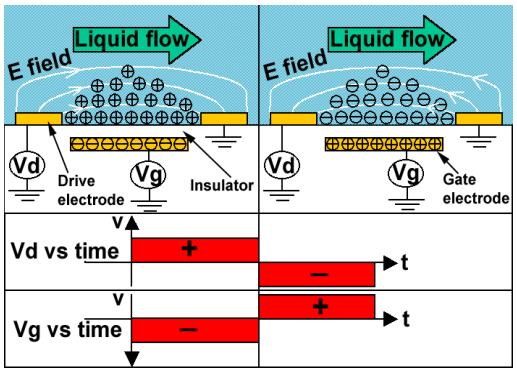

Fig. 7: Case showing affected charges, electric field and liquid flow direction when a periodic, net zero average waveform is applied to V_d and its negative to V_g. Net flow can be achieved as long as the *change* in the zeta potential is synchronous with V_d.

	Electric Field Direction	Affected Charges	Movement Direction	
Vd positive	+	+	+	Vg=-Vd
Vd negative	−	−	+	
Vd positive	+	−	−	Vg=Vd
Vd negative	−	+	−	
Vd positive	+	+	+	Vg floating
Vd negative	−	+	−	

Table 1: Different cases of a periodic net zero average waveform applied to driving voltage (V_d) and gate voltage (V_g).

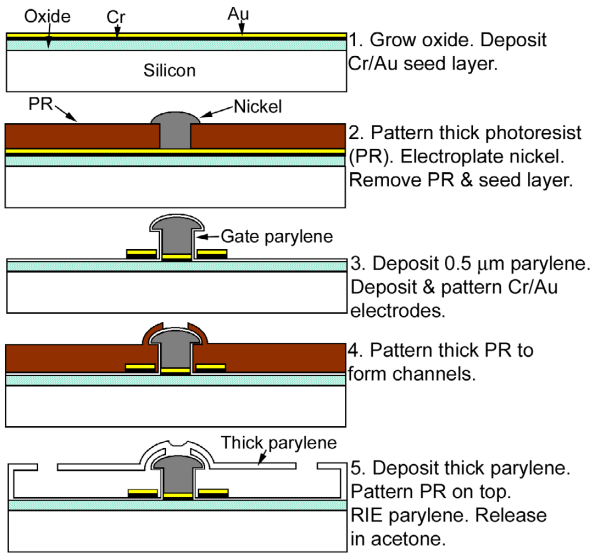

Fig. 8: Fabrication process for the flowFET.

The substrate is a silicon wafer with 2-µm thermal oxide. The device has a 20-µm high, 200-µm wide main channel. The gate electrode is formed by electroplating nickel through a 20-µm thick photoresist mold. The mold has 10 openings, 10-µm wide, 100-µm long, separated by 10-µm. The structure is over electroplated so that grown pillars will form mushroom structures forming closed channels [11]. A schematic of the final structure is shown in Fig. 6, forming 20-µm high, 10-µm wide 10 parallel channels. The electroplated channel array structure is conformally coated with 0.5-µm thick parylene. Figure 9 shows the fabricated device.

The total EOF velocity has two components: velocity due to zeta potential change and velocity due to natural zeta potential. A simple approximation to the effect of gate bias on zeta potential, ζ, under sinusoidal AC modulation is:

$$\Delta\zeta = \frac{C_{Wall}}{C_d}\left|V_g\right|\sin\omega \cdot t \qquad (3)$$

where ω is the frequency of the modulation voltage. This model assumes that the zeta potential is the potential at the intermediate node of a capacitive potential divider formed by the series combination of C_{Wall}, the capacitance due to the insulating coating and C_d, the double layer capacitance of the interface [8]. Assuming that the channel contains DI water with ion concentration of 7.5 µM and natural zeta potential of 30 mV, $|\Delta\zeta|$ is 62 mV for a V_g magnitude of 10 V, which is enough to reverse the polarity of the zeta

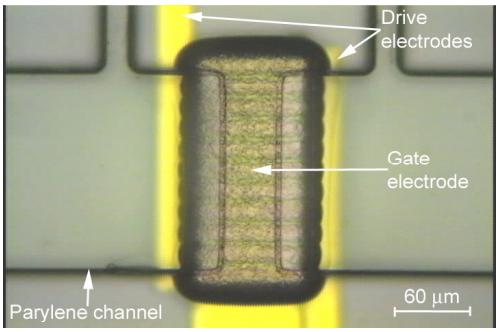

Fig. 9: Top view of the fabricated flowFET.

potential. For this channel dimensions the Helmholtz-Smoluchowski equation can be used to calculate EOF velocity, which is proportional to the zeta potential and the applied electric field. Therefore change in the EOF velocity due to zeta potential change is:

$$\Delta \upsilon_{eof} = \frac{\varepsilon \varepsilon_0}{\eta} \frac{|V_d|}{L} \frac{C_{Wall}}{C_d} |V_g| \sin^2 \omega \cdot t \qquad (4)$$

where V_d is the drive voltage, L the channel length, ε the dielectric constant of the medium and ε_0 the permittivity of free space. Integrating Eq. (4) over one cycle produces a net velocity. However the EOF velocity due to natural zeta potential yields net zero velocity.

For experimental verification, a 1 kHz square wave was applied to drive electrodes, and bead velocities were measured for three cases: the gate voltage floating, equal to V_d, and equal to $-V_d$, which resulted in no movement, forward and reverse movement of 1-μm latex microbeads, respectively, with bead velocities of up to 66 μm/s. Measurements were done in field-free regions after equalizing the pressures on both sides of the pump since with these channel dimensions pressure-driven flow can become dominant. The test results in Fig. 10 demonstrate the effectiveness of this concept.

R_{hyd} of 10 parallel narrow channels is 8.75×10^{12} Pa.s/m^3. With a signal magnitude of 16.6 volts, P_{max} =2.3 Pa. This low value is expected due to large dimensions of narrow channels. This can be improved easily by making width or height of narrow channels smaller than 1μm.

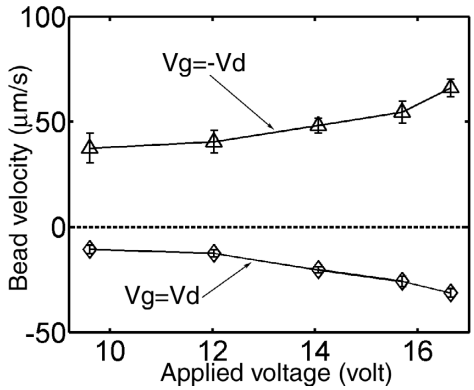

Fig. 10: Bead velocity vs. magnitude of V_d of a 1 KHz square wave, with V_g equals to V_d and $-V_d$.

VI. SUMMARY

This paper presents two alternative schemes for electrode placement and bias control for electro-osmotic pumping. The first scheme uses liquid bridge connections to the main channel through a porous polymer. In this manner, DC voltage could be applied without causing any bubble generation in the main channel. At 50 V DC, the flow rate was 1.76 nL/min. The second scheme rectifies AC driven electro-osmotic flow by zeta potential modulation of surfaces of a high aspect-ratio perforated gate electrode covered with a thin insulator. Using a square wave of 16.6 V at 1 kHz applied to driving electrodes, latex microbeads showed a velocity of 66 μm/s if the gate voltage was the negative of the driving voltage, and a reverse velocity of 31 μm/s if it was the same polarity.

ACKNOWLEDGEMENTS

This work was supported by DARPA under grant F30602-00-1-0571.

REFERENCES

[1] C.H. Chen, J.G. Santiago, "A Planar Electroosmotic Micropump," *Journal of Microelectromechanical Systems*, vol. 11, pp. 672-683, 2002

[2] C.L. Rice, R. Whitehead, "Electrokinetic Flow in a Narrow Cylindrical Capillary," *The Journal of Physical Chemistry*, vol. 69, pp.4017-4024, 1965.

[3] S. Mutlu, C. Yu, P. Selvaganapathy, F. Svec, C.H. Mastrangelo, J.M.J. Frechet, "Micromachined porous polymer for bubble free electroosmotic pump," *Proc. IEEE MEMS'02*, pp. 19-23, 2002.

[4] K.J. Vetter, *Electrochemical Kinetics*, Academic Press, 1967.

[5] Y. Takamura, H. Onoda, H. Inokuchi, S. Adachi, A. Oki, Y. Horiike, "Low-voltage electroosmosis pump for stand-alone microfluidics devices," *Electrophoresis*, vol. 24, pp. 185-192, 2003.

[6] J.P. Alarie, S.C. Jacobson, B.C. Broyles, T.E. McKnight, C.T. Culbertson, J.M. Ramsey, "Electroosmotically induced hydraulic pumping on microchips," *Tech. Dig., μTAS,* 2001, pp. 131-132.

[7] S. Zeng, C.H. Chen, J.C. Mikkelsen Jr., J.G. Santiago, "Fabrication and Characterization of Electroosmotic Micropumps," *Sensors and Actuators B*, vol. 79, pp. 107-114, 2001.

[8] R.B.M. Schasfoort, S. Schlautmann, J. Hendrikse, A.V.D. Berg, "Field-effect flow control for microfabricated fluidic networks," *Science,* vol. 286, pp. 942-944, 1999.

[9] P. K. Wong, C.-Y. Chen, T.-H. Wang, C.-H. Ho, "An AC electroosmotic processor for biomolecules," *Proc. Transducers'03*, Boston, pp. 20-23, 2003.

[10] E.V. Dose, G. Guiocchon, "Timescales of transient processes in capillary electrophoresis," *Journal of Chromatography A*, vol. 652, pp. 263-275, 1993.

[11] Y. Joo, K Dieu, C.J. Kim, "Fabrication of monolithic microchannels for IC chip cooling," *Proc. IEEE MEMS'95*, pp. 362-367, 1995.